SAE International

2013-01-1250
Published 04/08/2013

doi:10.4271/2013-01-1250
saepcmech.saejournals.org

Evaluation of the Aerodynamic and Aeroacoustic Response of a Vehicle to Transient Flow Conditions

Nicholas Oettle, Oliver Mankowski, David Sims-Williams and Robert Dominy
Durham University

Claire Freeman
Jaguar Land Rover

ABSTRACT

A vehicle on the road encounters an unsteady flow due to turbulence in the natural wind, unsteady wakes of other vehicles and as a result of traversing through the stationary wakes of roadside obstacles. Unsteady effects occurring in the sideglass region of a vehicle are particularly relevant to wind noise. This is a region close to the driver and dominated by separated flow structures from the A-pillar and door mirrors, which are sensitive to unsteadiness in the onset flow. Since the sideglass region is of particular aeroacoustic importance, the paper seeks to determine what impact these unsteady effects have on the sources of aeroacoustic noise as measured inside the passenger compartment, in addition to the flow structures in this region. Data presented were obtained during on-road measurement campaigns using two instrumented vehicles, as well as from aeroacoustic wind tunnel tests.

Conventional admittance functions relating oncoming flow yaw angle to cabin noise response are generally not suitable due to the non-linear steady state characteristics obtained in the wind tunnel, i.e. the cabin noise does not vary with yaw angle in a linear fashion under steady-state conditions. Therefore two alternative approaches were used based on instantaneous conditions to determine a quasi-steady predicted cabin noise time-history. These techniques demonstrated that the cabin noise response to oncoming flow unsteadiness remained generally quasi-steady up to fluctuation frequencies of approximately 2 to 5 Hz, where above this smaller flow scales have a progressively smaller impact on cabin noise fluctuations. Therefore, with a measurement of both the cabin noise in the steady environment of the wind tunnel and the unsteady onset flow conditions, the fluctuations (and thus the modulation) of the wind noise under these unsteady conditions is able to be predicted.

CITATION: Oettle, N., Mankowski, O., Sims-Williams, D., Dominy, R. et al., "Evaluation of the Aerodynamic and Aeroacoustic Response of a Vehicle to Transient Flow Conditions," *SAE Int. J. Passeng. Cars - Mech. Syst.* 6(1):2013, doi: 10.4271/2013-01-1250.

INTRODUCTION

A vehicle on the road encounters an unsteady flow due to turbulence in the natural wind, unsteady wakes of other vehicles and as a result of traversing through the stationary wakes of roadside obstacles. These various sources of oncoming flow unsteadiness and their effects have been investigated by various researchers including [1, 2, 3, 4, 5, 6] and are summarised by Sims-Williams (2011) [7]. Previous work on unsteady on-road effects on aeroacoustics has been published by [8, 9, 10, 11, 12].

Unsteady effects occurring in the sideglass region of a vehicle are particularly relevant to wind noise. This is a region close to the driver and dominated by separated flow structures from the A-pillar and door mirrors, which are particularly sensitive to unsteadiness in the onset flow.

Previously, work by Oettle et al. (2012) [10] showed that deviations in the sideglass surface pressure distribution from that predicted under steady-state condition can occur, isolated particularly to the region nearest the A-pillar under leeward flow conditions. This work extends that investigation, determining the transient sideglass surface pressure response for an alternative vehicle geometry, seeking to determine what impact these unsteady effects have on the aeroacoustic noise inside the passenger compartment as well as on the vehicle exterior.

EXPERIMENTAL METHOD

Two vehicles were used during the course of experimentation, recording data relating to cabin noise and sideglass surface pressures respectively. In addition to either the surface pressures or cabin noise, a roof-mounted probe was incorporated to record the instantaneous oncoming flow conditions.

Test Vehicles

A vehicle typical of a European luxury saloon was used as the test vehicle, shown in Figure 1 and was the same model as used in the previous research of Oettle (2013) [13] incorporating Oettle et al. (2012, 2011, 2010) [10,11,12]. As shown, a probe was mounted on the roof of the vehicle for the measurement of instantaneous flow conditions. The coordinate system that is used throughout the paper is shown in Figure 1 and Figure 2.

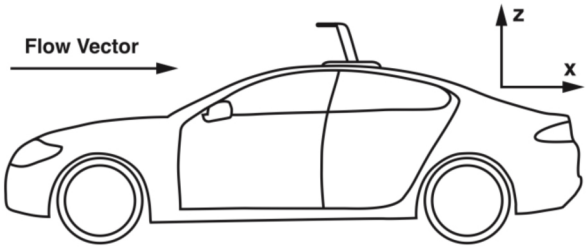

Figure 1. Test vehicle showing location of probe

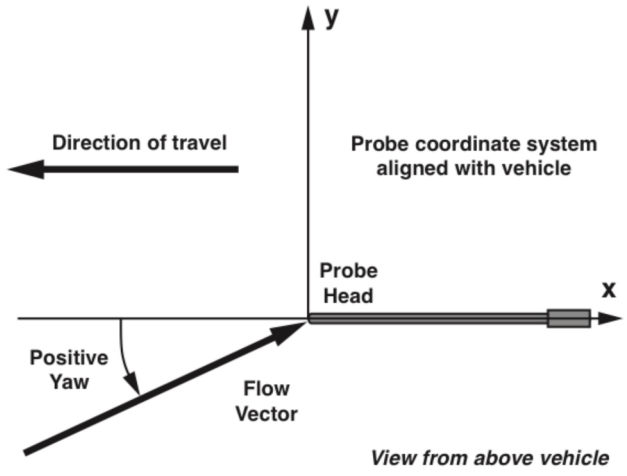

Figure 2. Plan view: Probe and vehicle coordinate system

Surface pressure investigations were also performed the European two box hatchback vehicle described by Lawson et al. (2007) [14]. The same roof-mounted probe as corresponding coordinate system was used as with the cabin noise measurements.

On-Road Data Collection

Roof Mounted Probe

To measure the flow over both vehicles, a roof-mounted 5-hole probe was used, as in Oettle (2013) [13]. The probe tip was positioned approximately 320 mm above the vehicle's roofline, and approximately 70 mm in front of the B-pillar, as shown in Figure 1. The probe was manufactured and calibrated in isolation using facilities at Durham University. Five SensorTechnics HCLA12X5DB pressure transducers were used to measure the probe pressures. These measure differential pressure and have a range of ±12.5 mbar. The transducers were packaged into a single enclosure with a common reference and located within the probe mounting. The reference port was connected via a PVC tube to a location in the trunk of the vehicle. The probe mounting was attached to the roof of the vehicle magnetically.

A probe and tubing transfer function correction was applied, for magnitude and phase, to all on-road data for both the roof mounted five-hole probe and the sideglass pressure tappings. This is described by Irwin et al. (1979) [15] and implemented for probe measurements here as described by Sims-Williams and Dominy (1998) [16]. With the probe and remote transducers used in the investigation, this approach allows a frequency response in excess of 500 Hz. This significantly exceeds the required response for this application as higher frequency fluctuations contained in the wind are also correspondingly small in physical size and are therefore not correlated over the scale of the vehicle.

Any probe installation location will be a compromise between measuring the incoming flow that the vehicles sees, minimizing the influence of the probe on the flow around the vehicle, and minimizing the influence of the vehicle on the flow at the probe.

It was important for the design of the probe mounting not to have a significant impact on the flow at the probe tip or to affect flow around the vehicle in either the sideglass region or in other areas that may affect the noise heard inside the cabin. In addition, it was important that the probe had a minor impact on aeroacoustic measurements.

The approach used here (e.g. positioning the probe some distance off the vehicle and using a probe calibration performed in isolation rather than in situ) means that the yaw angles and other quantities reported are the actual values at the probe location and this is known with certainty. Steady state wind tunnel measurements show that the probe experiences a speed up of both longitudinal and lateral velocity components. This has been shown to be a good probe location for accurate measurement of yaw [13], although the yaw angle seen by the probe still becomes slightly exaggerated at higher yaw angles. While it may be tempting to “correct” for these effects that would assume that the flow around the vehicle in a transient condition matches that in the steady state condition. This investigation concerns the comparison between the aerodynamic response of the

vehicle under steady state and transient conditions and so such an assumption would not be appropriate a priori.

Sideglass Pressures

Surface pressures were measured on the front sideglass using both surface-mounted "lollipop" taps on the standard glass sideglass as described by [14], and using a drilled Perspex sideglass moulded to the shape of the production glass with 1.24 mm OD hypodermic stainless steel tubing bonded in position. Pressures were measured using separate SensorTechnics HCLA12X5DB pressure transducers located inside the cabin connected to each surface taping via PVC tubing. As for the probe measurement, pressures were measured relative to trunk pressure. Pressure coefficient CP was defined based on the static and dynamic pressure measured by the 5-hole probe. Again this provides something that is known with certainty in the on-road case as well as in the wind tunnel.

$$c_P = \frac{P_{\text{Tap}} - P_{\text{Probe Static}}}{\frac{1}{2}\rho U^2_{\text{Probe Resultant}}}$$

Data Acquisition

To log the output from the pressure transducers, a National Instruments NIDAQmx USB-6218 data logger was used. This was controlled by a laptop running control software developed in-house. Data were also received from a GPS device that was simultaneously logged with the pressure transducer data from the data logger using the same control software. The GPS data included details of the velocity and heading of the vehicle, in addition to information on the location of the vehicle and time of the experiment. The pressure transducer data were logged in sets of 16384 points at 500 Hz, therefore giving a logging duration of 32.768 s. This logging time was considered suitable to capture the transient nature of the on-road environment. To avoid aliasing, the signal from each of the pressure transducers was passed through a 250 Hz second-order low-pass filter.

Cabin Noise Measurement

A Head Acoustics Aachen head with torso was used to record the cabin noise. This was positioned on the front left (passenger) seat of the vehicle and fixed securely to prevent any additional noise generation. The ventilation system was switched off during testing.

The acoustic head was connected to the logging computer via a Head Acoustics front-end and controlled through the Head Acoustics HEAD Recorder software. Logging took place at 44.1 kHz. In addition to the combined trigger for both flow and audio logging systems, a 2 kHz tone was generated and silenced at the point of logging to assist synchronising the logging systems with a simultaneous video recording.

Head Acoustics ArtemiS software was used to extract SPL (sound pressure level) from the audio data collected both on-road and in the wind tunnel.

Wind Tunnel

The Pininfarina wind tunnel was used to assess the cabin noise response of the vehicle to discrete steady-state flow conditions. Instrumentation remained the same as for on-road data collection. The results reported here were obtained using a stationary ground boundary condition and static wheels. The results reported here were obtained using a stationary ground and wheels and without the Pininfarina turbulence generation system. Measurements were made at a range of turntable yaw angles from −20 degrees to +20 degrees at 2.5 degree increments. The nominal wind tunnel velocity matched the on-road driving velocity. As discussed above, the yaw angles reported in the results correspond to those measured at the probe since this is what is always known with certainty.

The steady-state surface pressure coefficient versus yaw characteristics were obtained via wind tunnel measurements and by conditional averaging of on-road measurements. While differences could be observed between these two approaches in some cases from the point of view of time-averaged C_P, both methodologies for determining the steady-state characteristics yielded the same conclusions in terms of the vehicle's transient response.

RESULTS AND DISCUSSION

Typical Admittance and Transfer Function Approaches

The aerodynamic admittance is a common method used to quantify the aerodynamic response of a vehicle to unsteadiness. This is usually defined for aerodynamic coefficients, but there is no reason why may not be defined in terms of aeroacoustic admittance, as in the following equation:

$$\chi\left(f\right)^2 = \frac{G_{LL}\left(f\right)}{\left(\frac{\mathrm{d}L}{\mathrm{d}\psi}\right)^2 G_{\psi\psi}\left(f\right)}$$

This is similar to a transfer function defined as the ratio between the SPL and yaw angle spectra. As f tends to zero, it would be expected that the admittance would tend to unity, with the transfer function tending to the sensitivity of changes in SPL to yaw angle measured under the steady conditions of the wind tunnel. Both approaches are shown in general terms by Figure 3 where the oncoming flow conditions are described by F(t) and the vehicle response by R(t).

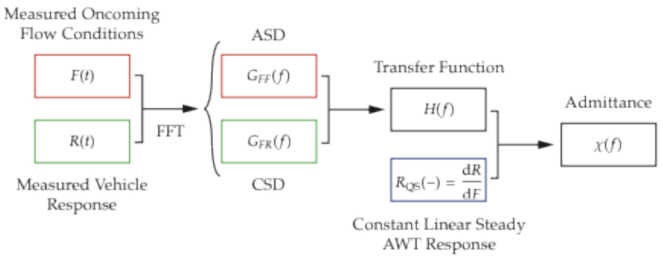

Figure 3. Method to determine the transient response of a vehicle via admittance

When considering aerodynamic admittance, for example based on a side force or yaw moment coefficient on a vehicle, the coefficients tend to vary linearly with yaw angle. Therefore, the rate of change (gradient) between the force coefficients and yaw remains independent of the particular instantaneous oncoming yaw angle.

However, when considering localised surface pressure changes, for instance the pressure at a particular point on the sideglass, see Oettle et al. (2012) [10], the behaviour may not be linear, for instance on the sideglass region adjacent to the A-pillar. This is also particularly the case when considering the response of cabin noise to yaw angle, where it is clear that owing to the greater amount of flow separation at the extremes of yaw angle, that the cabin noise at both positive and negative yaw angles is greater than at a zero yaw condition. Therefore the cabin noise is not at all linear with yaw angle and therefore an equivalent aeroacoustic admittance approach would not be appropriate. Indeed, when determining the aeroacoustic admittance on-road, this term would vary depending on the range of yaw angles experienced.

Cabin noise is not only affected by variations in oncoming yaw angle, but also to fluctuations in flow speed. Typically the relationship between oncoming flow speed and cabin noise scales with oncoming flow speed raised to the power of the order of 6, indicating dipole dominated aeroacoustic sources. Therefore, instead of a single input - single output system, a multiple input - single output system must be considered, discussed in further detail by Bendat and Piersol (1993) [17]. This does not preclude such a transfer function assessment *per se*, it is the non-linear response of cabin noise to yaw angle which provides the challenge, as it could be imagined that the logarithmic response of the cabin noise to flow speed could be successfully linearized.

Therefore an alternative approach was sought to be able to assess the response of the vehicle to fluctuations in the oncoming flow when the steady-state response is non-linear.

An Alternative Linearized Transfer Function Approach

To assess the nature of the vehicle cabin noise response, a simulation technique was implemented which used the cabin noise response to both oncoming yaw and flow speed measured in the wind tunnel, combined with the measured transient flow characteristics measured by the probe on the vehicle roof on-road to predict the instantaneous sideglass pressure. This directly compares the behavior of the vehicle on-road to that predicted by the wind tunnel. Therefore any non-linearities in the wind tunnel steady-state characteristics are removed and converted into a continuous predicted time-history of cabin noise. In the case of localized sideglass surface pressure tappings, this technique was previously introduced by Oettle (2012) [10]. Figure 4 outlines a generalized form of this process.

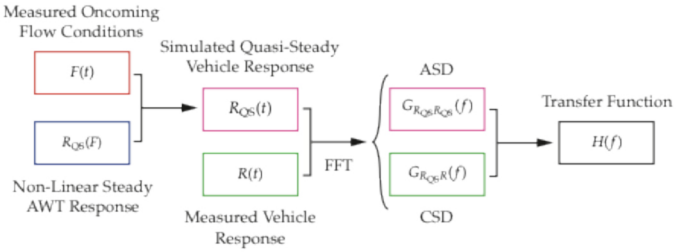

Figure 4. Method to determine the transient response of a vehicle via a linearized approach

This process results in a transfer function whereby a value of unity implies that the vehicle response to oncoming flow fluctuations is equal to that predicted in the steady environment of the AWT i.e. the response is quasi-steady. A transfer function of greater than unity implies that the vehicle responds to a greater extent that predicted by the instantaneous oncoming flow conditions alone, whilst a response of less than unity implies a response less than predicted under steady conditions.

It has been shown, for instance by Schröck (2009) [18] that for the aerodynamic response of a vehicle, a transfer function of unity would be expected at lower frequencies for scales much greater than the vehicle, where the response can be considered to be quasi-steady. At higher frequencies, the vehicle response is no longer quasi-steady, although the higher-frequency, small-scale fluctuations much smaller than the size of the vehicle have a progressively decreasing impact of the vehicle response, leading to a transfer function of less than unity. In the intermediate frequency range, scales of unsteadiness may exist that are sufficiently large and of sufficient energy to influence a vehicle, but not so large that they can be considered to be quasi-steady. This is discussed further in Sims-Williams [7]. These effects can lead to transfer function values of greater than unity and these are sometimes associated with resonances of the vehicle suspension system in the case of vehicle forces.

The alternative linearized approach simplifies the analysis of the system, since multiple-input problems can be simplified to consider only a single input, avoiding the need for a multiple input - single output analysis. For instance, it has been shown that the noise inside the cabin of a vehicle is influenced by both the oncoming flow speed and yaw angle. Instead of assessing these as independent inputs to the

system, these inputs are linearized to produce a single input of the expected cabin noise as determined under the steady conditions of the wind tunnel. This single input is then assessed against the single output of the measured cabin noise to determine the response of the system.

Steady-State Characteristics

The steady-state wind tunnel obtained overall cabin noise SPL response characteristic is shown in *Figure* 5. This presents the overall cabin noise measured at the left-head, left-ear position at a series of yaw angles and flow speeds in the wind tunnel.

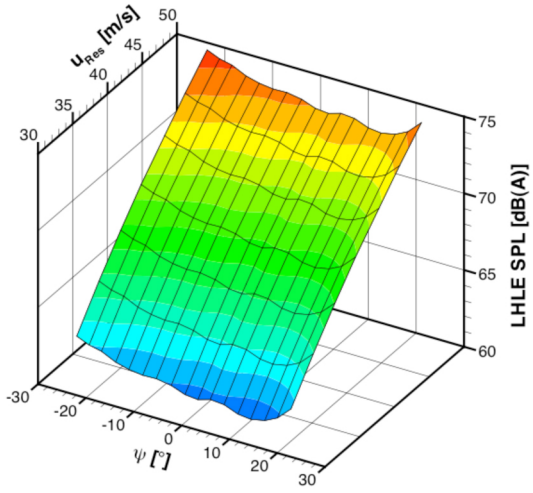

Figure 5. AWT cabin noise characteristic

This is a compound surface of the yaw and flow speed cabin noise characteristics determined in the AWT. In producing the surface, multiple yaw sweeps and a zero-yaw speed sweep were combined to produce an overall surface, with interpolation used for the behaviour between the measured conditions. In addition to the overall level, characteristics of the various third-octave frequency bands of cabin noise were also produced using the same AWT data.

For surface pressures only a pressure coefficient versus yaw characteristic is required. These were obtained from wind tunnel measurements and by conditional averaging of on-road measurements and both approaches yielded the same conclusions in terms of the vehicle's transient response.

For the case of the sideglass pressure tapping data, instead of determining the steady-state response in the wind tunnel, the time-averaged response was used. This method used a 2.5° spaced Bin Average process to take each and every 4 seconds period of the on-road 5-hole probe sampled data from a collection of 252 × 32s data. The time-averaged pressure coefficient was then evaluated for each sideglass tapping per bin, with the central bin located at $^{+}/_{-}1.25°$, and the average flow yaw angle for each sample used as the actual bin yaw angle (i.e. the independent variable for subsequent simulation).

The resultant output file from this process was a time-averaged pressure coefficient against averaged flow yaw angle at 2.5° intervals for each sideglass tapping, between $^{+}/_{-}22°$. An example of the output of this method can be seen in *Figure* 6 for 3 sideglass tappings.

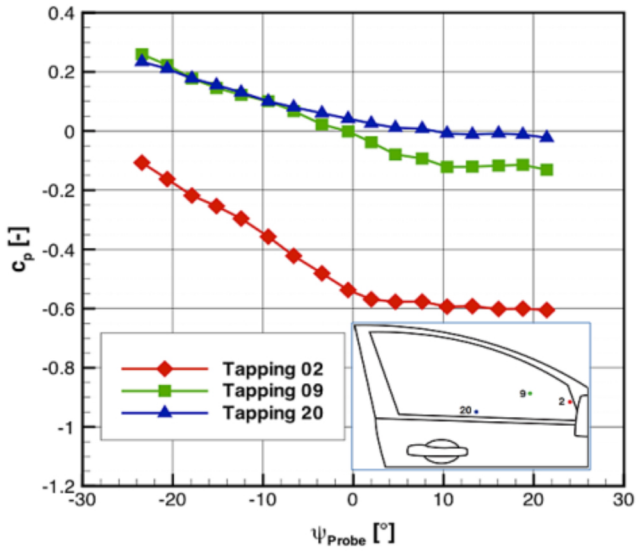

Figure 6. Pressure Coefficient against Flow Yaw Angle (Bin Averaged)

Experimental Prediction and Transfer Functions

To create the overall transfer function comparing both the measured and quasi-steady predicted sideglass pressure fluctuation, the time-averaged sideglass pressure tapping characteristics were first combined with the probe measured oncoming flow conditions for each of the sets of on-road data collected. This results in a quasi-steady simulated time-history that can be compared with the equivalent on-road measured pressure tapping fluctuations. A comparison between these two signals is shown in ***Figure*** 7 reproduced from Oettle et al. (2012) [10], showing a visually good agreement between the transient on-road data and the wind tunnel quasi-steady predicted result.

The first observation is that the agreement is very good, with the behaviour at the scales that are visible on a 30s time trace being closely quasi-steady. It is, of course, difficult to assess frequencies much higher than 1 Hz in this way and so further analysis is required to assess the vehicle response at higher frequencies. It is possible to calculate a transfer function between the predicted and measured traces and this provides some insight, but the transfer function becomes corrupted by any self-excited effects. This was discussed and demonstrated in Oettle et al. (2012) [10]. A better approach is to compare the measured level of unsteadiness over a short duration (e.g.: 4s) with the corresponding predicted level of unsteadiness (which is a prediction of surface pressure unsteadiness due only to unsteadiness in the oncoming flow).

By bandpass filtering the unsteadiness it is possible see how the comparison varies with frequency, as in *Figure* 8.

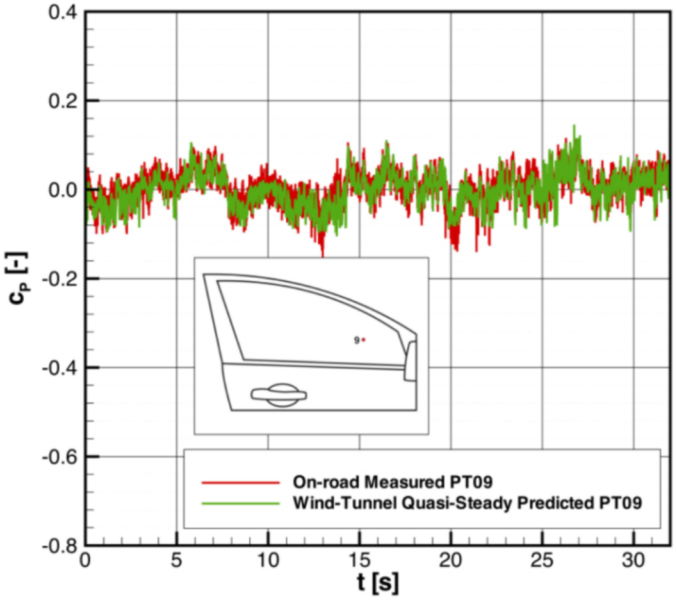

Figure 7. Example surface pressure trace measured on-road and quasi-steady prediction from wind tunnel test and measured transient yaw. (from Oettle et al 2012).

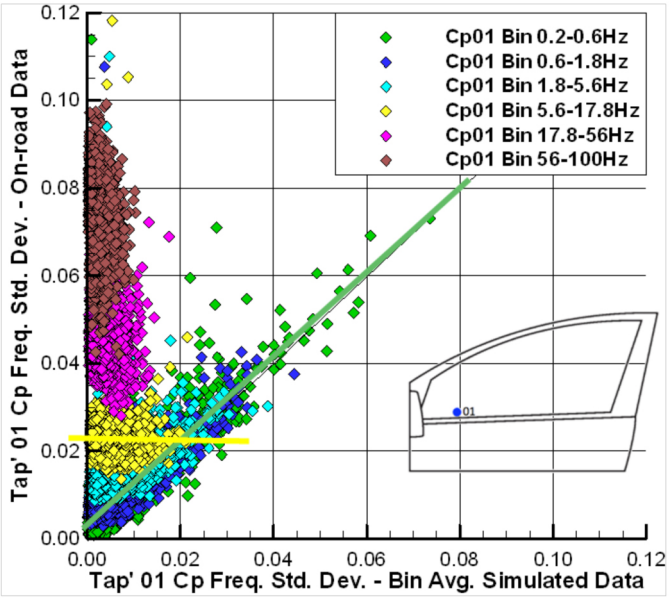

Figure 8. Comparison between surface pressure unsteadiness measured and predicted using quasi-steady method.

A conventional transfer function at a given frequency would be the slope of a line drawn on this figure between the origin and the middle of the cluster of points representing that frequency. Inspecting the figure we see that at low frequencies a best fit straight line has a slope of approximately unity and zero intercept value, indicating that the surface pressure unsteadiness is strongly correlated with the quasi-steady prediction, indicating that the response is quasi-steady and that the surface pressure unsteadiness is dominated by the unsteadiness (yaw variation) in the incoming flow. However, at higher frequencies the surface pressure unsteadiness is no longer correlated with that which would be predicted from the yaw variation and the response is characterised by a near zero slope and non-zero intercept; the latter representing the level of self-excited unsteadiness.

From a simple linear fit to the scatter of points for each frequency we can obtain a better assessment of the transfer function or admittance function from the respective slopes and we can extract the level of self-excited unsteadiness from the intercepts, illustrated in ***Figure*** 9 and ***Figure*** 10 respectively.

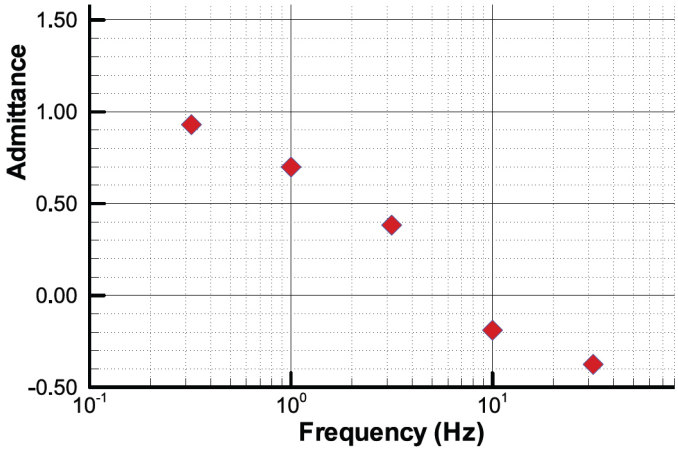

Figure 9. Mirror wake region true admittance function (transfer function) between the quasi-steady prediction and actual vehicle response measured on-road using the "slope and intercept method"

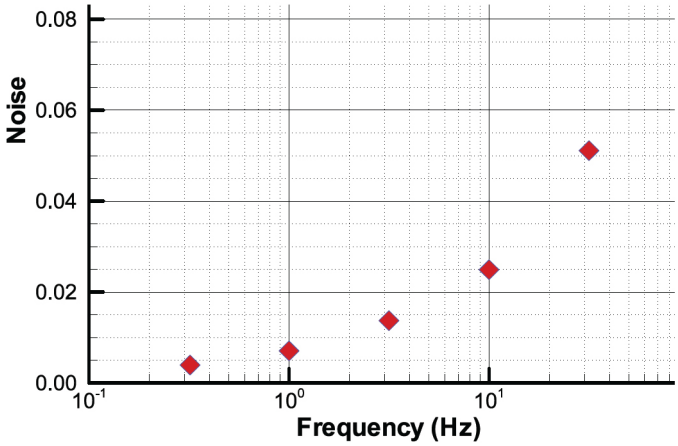

Figure 10. Mirror wake region self-excited unsteadiness for each frequency band determined from vertical axis intercepts.

Throughout the mirror wake region the admittance function is similar, with an admittance approaching unity at the lowest frequencies (~0.2 Hz) and reducing to near zero admittance by about 10 Hz. Very close to the A-Pillar admittance greater than unity was observed for some frequencies and self-excited unsteadiness was much less dominant. Similar results were obtained for both vehicles investigated.

A similar approach to the surface pressure data was completed for the cabin noise data. In generating the steady-state predicted cabin noise fluctuations, the AWT-predicted cabin noise characteristic for each individual third-octave band was used to determine the cabin noise fluctuation for that particular band for a given on-road measured oncoming flow fluctuation. The result of this process is shown in Figure 11, where a short example on-road time history is used to compare the measured cabin noise and the quasi-steady predicted cabin noise for the 4 kHz third-octave frequency band.

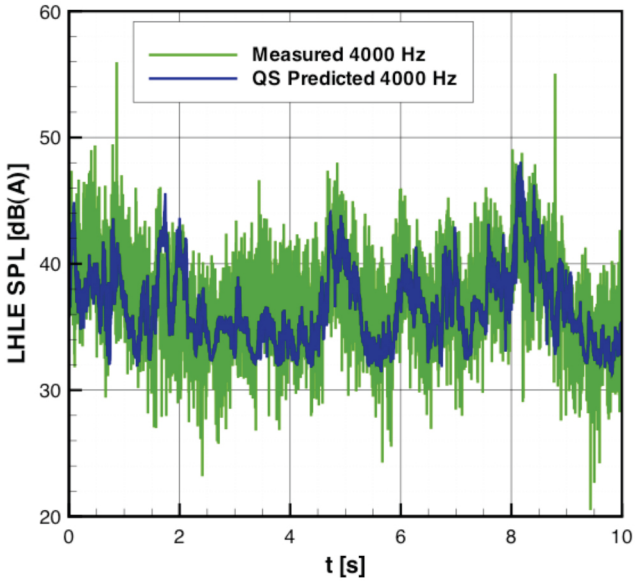

Figure 11. Temporal comparison between measured and quasi-steady predicted cabin noise (4 kHz third-octave band)

For this data, it is shown that the predictive technique captures the overall shape of the measured time-history well, with both the overall level and size of the larger fluctuations with relative accuracy. This indicates that not only does the predictive model work well, but also that the longer fluctuations in the measured cabin noise are indeed due to variations in the oncoming flow which are measured by the roof-mounted probe. The most significant difference between the two signals is the level of additional higher-frequency modulation present in the measured on-road cabin noise, which is not present in the quasi-steady prediction. This indicates that there is a level of high frequency fluctuations heard inside the cabin not due to fluctuations in the oncoming flow.

This is the same phenomenon as found when assessing the surface sideglass pressure fluctuations and is due to self-excited unsteadiness independent of the oncoming flow unsteadiness passing over the vehicle. Sideglass noise is a key component of the noise heard inside the cabin and this is related to surface pressure through the following relationships. The link between localised flow speed and surface pressure is given by George (1990) [19] and is described in the following equation showing the relationship between local flow speed u, free-stream flow speed u_∞ and surface pressure coefficient C_P.

$$\left(\frac{u}{u_\infty}\right)^6 = \left(1 - c_p\right)^3$$

This relationship is shown with the flow speed ratio raised to the sixth power, as would be the case when relating this ratio to a change in SPL for a pure dipole source. The relationship between C_P and SPL increase then simply follows, highlighting the impact of a change of local flow speed on a dipole wind noise source.

$$\Delta\mathrm{SPL} = 10\log\left(\frac{u}{u_\infty}\right)^6 = 10\log\left(1 - c_p\right)^3$$

To further demonstrate the self-excited content, the transfer function approach was continued, with the appropriate spectral densities of the two signals determined using the complete set of on-road measured time-histories. The resulting transfer function for a selection of third-octave bands is presented by Figure 12.

The third-octave bands chosen comprise two different sets of sources. The band centred at 800 Hz is dominated by road noise emanating from the contact of the tyres on the road surface. Therefore whilst this band does contain some aeroacoustic content, the fluctuations of this frequency band are primarily due to changes in the road surface, rather than fluctuations in the oncoming flow conditions. Conversely, the 4, 6.3 and 8 kHz bands are dominated by wind noise sources.

For each of these wind-noise dominated bands, the magnitude of the transfer function up to approximately 5 Hz remains close to unity, indicating quasi-steady behaviour, as shown by Figure 12. Above this frequency, the transfer function magnitudes rise rapidly, indicating that there is increased high frequency energy contained within the measured cabin noise signal, but not in the AWT quasi-steady predicted signal.

The road-noise-dominated 800 Hz band behaves differently to the wind noise dominated bands at lower frequencies, in that the lowest frequency point is greater than unity, indicating that the steady-state (time-averaged) SPL is greater on-road than predicted in the AWT. This difference is due to the road noise not present in the AWT. At higher frequencies, the transfer function magnitude drops below

unity, indicating a reduced level of ~800Hz fluctuations heard in the cabin than predicted from the oncoming flow unsteadiness. This is due to aeroacoustic fluctuations being acoustically masked by the dominant road noise as heard inside the cabin.

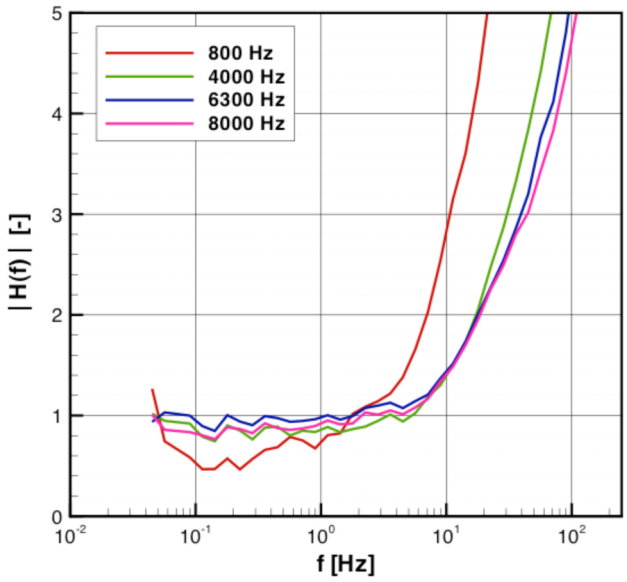

Figure 12. Transfer functions between measured and quasi-steady predicted cabin noise

It would be expected that at higher fluctuation frequencies, the magnitude of the transfer functions would gradually decrease, as the smaller fluctuations of the oncoming flow unsteadiness have a progressively reducing impact on fluctuations in noise as heard inside the cabin. However, as also identified by the sideglass surface pressure measurements, the cabin noise fluctuations heard inside the vehicle are not solely due to fluctuations in the oncoming flow. Self-excited unsteadiness from the various vehicle geometry scales, ranging from the bluff body of the vehicle itself to the smaller components such as the mirrors and windscreen wipers lead to an ensemble of scales and fluctuation frequencies. These self-excited effects lead to fluctuations of the various cabin noise frequency bands and are ultimately the cause of having to record the cabin noise in the AWT for a period of time before averaging to determine the SPL at a given vehicle condition. These fluctuations are removed during this averaging process and thus are not captured by the AWT-determined steady-state cabin noise characteristic.

A rudimentary assessment of the minimum frequency that would be affected by these self-excited effects can be determined using the Strouhl number (St). By assuming St=0.21, the nominal flow speed as u=36.1 m/s and a maximum characteristic length of the square root of vehicle frontal area (where A_f=2.33 m^2) leads to a minimum self-excited fluctuation frequency of approximately 5 Hz as shown by the following equation. This is consistent with the rapid rise in transfer function magnitude as shown by Figure 12.

$$f = \frac{\mathrm{St} \cdot u}{\sqrt{A_f}} = 5 \text{ Hz}$$

Overall, this linearized transfer function approach provides useful information as to the response of the vehicle to fluctuations in the oncoming flow. This section has demonstrated that the linearized transfer function approach may be used to assess the nature of the vehicle response in a fluctuation frequency range when self-excited effects are not present. This has demonstrated that the flow structures around the sideglass region generally remain quasi-steady up to between 2-5 Hz, where self-excited effects begin to dominate. An exception to this is in the region close to the A-pillar, where the admittance increases to values greater than unity in the 10 Hz frequency range, seemingly independent of any self-excited effects. The sideglass surface pressure response is similar for both the premium saloon as presented by Oettle et al. (2012) [10] and also for the smaller hatchback vehicle in this paper, indicating that this response is consistent between different vehicle geometries.

The key disadvantage of this technique is that it does not naturally separate the effects of the oncoming flow unsteadiness from self-excited effects. The following section introduces an alternative technique, focussing on the cabin noise response, to remove the self-excited effects present in the transfer function.

Broadband Modulation Approach

The previous linearized technique involves modulating the time-averaged cabin noise and comparing this to the time-varying cabin noise measured on-road. Thus the self-excited content is present in the on-road data whilst it is removed during the time-averaging operation in the AWT. This is equivalent to taking a time history of a constant level, determined in the AWT at a zero yaw, nominal flow speed condition, and increasing or decreasing this level based on the steady AWT characteristic of Figure 5. This process is shown by Figure 13.

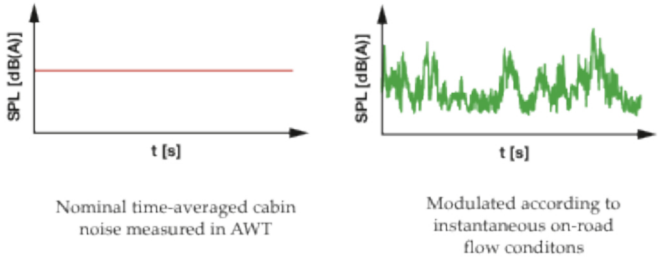

Figure 13. Cabin noise simulation using time-averaged characteristic alone

If instead of using the time-averaged SPL determined in the AWT, the time-varying SPL signal was used and modulated according to the AWT characteristic as before, this allows the self-excited frequency content to be captured in addition to the response due to oncoming flow unsteadiness. These self-excited effects are then included in both the on-road measured and quasi-steady predicted cabin noise signals, allowing these effects to be cancelled out in calculating the transfer function. This process is shown in ***Figure*** 14. This effectively uses the fluctuations as predicted in the AWT as the modulation envelope for the nominal cabin noise signal as recorded in the AWT.

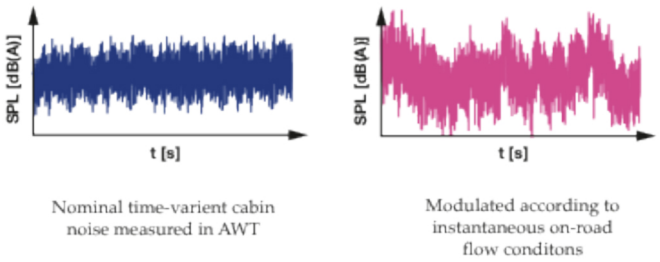

Figure 14. Cabin noise simulation through modulation of the time-variant cabin noise

The key difference between this broadband technique and the alternative linearized technique using the time-averaged characteristic alone is that the characteristic is used to determine the increase in SPL from the SPL measured in the nominal zero yaw, 36.1 m/s vehicle speed condition. This signal is then used to modulate the overall level of the cabin noise recorded in the AWT under these nominal conditions. This technique is analogous to amplitude modulation in radio transmission. The modulation was completed using a C-language routine that read in the nominal AWT cabin noise as a Wave (*.wav) file and modulated the signal. Linear interpolation was used to upscale the sampling frequency of the measured flow data to match that of the audio data. A new Wave file was then produced and processed in an identical manner to the on-road measured cabin noise files, allowing the third-octave frequency bands of SPL to be extracted. A convenient by-product of this approach is that an audio file of the simulated wind noise is produced, allowing subjective listening studies to take place on various wind conditions and vehicle characteristics.

The previous process took the AWT characteristics for each third-octave band and predicted how each band would fluctuate based on the oncoming flow conditions. This broadband technique uses the overall SPL characteristic and modulates the nominal cabin noise signal without differentiating between the various third-octave frequency bands.

One advantage of the broadband approach is that it is relatively simple to implement, with all processing taking place in the time domain. Therefore the modulation of the sound file can be completed instantaneously, with no delays in processing. This would be an advantage when instantaneously generating wind noise for use in, for example, a driving simulator. This would allow the wind noise to be simulated based on the deterministic input of a driver based on a vehicle speed or location (and hence wind condition) input.

The fundamental disadvantage of a broadband technique is that it assumes a consistent response over the entire frequency range. To assess the validity of this technique in capturing the behaviour of the key wind noise third-octave frequency bands, the variation of these bands was compared against the overall SPL as both the flow speed and yaw angle was varied in the AWT. An equal SPL increase of both a third-octave band and the overall SPL would imply that the broadband modulation technique models that particular band well. If the increase in SPL is different, this band will experience either an over or under amplification with the broadband technique. The results of this process are presented, with Figure 15 showing the relationship between a number of key third-octave bands and the overall SPL as the flow speed is increased in the AWT. The diagonal gridlines indicate an equal overall SPL to third-octave ratio.

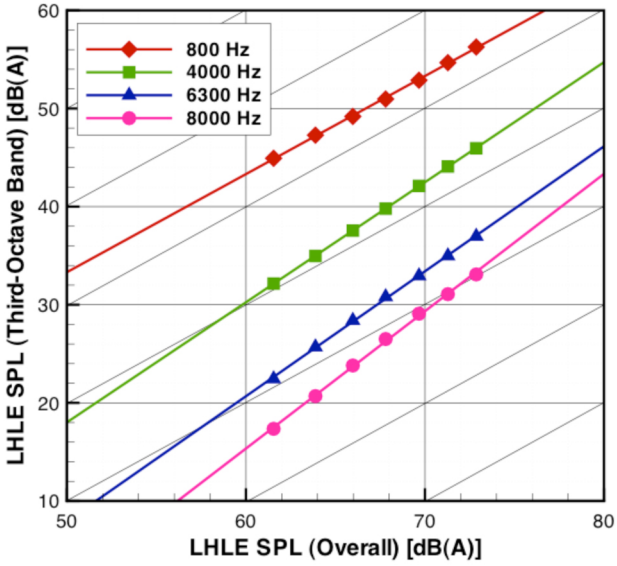

Figure 15. Comparison between third-octave and overall SPL under changes to resultant flow speed in AWT

The same four key third-octave bands are shown as in Figure 12 when presenting the transfer functions using the previous technique. For variations in flow speed as shown by Figure 15, the higher frequency third-octave bands show an increased sensitivity to flow speed, where the vehicle responds more greatly to changes in flow speed at these higher frequencies than the overall SPL. Therefore a broadband modulation technique will tend to underestimate these higher frequency fluctuations. Whilst the 800 Hz third-octave band shows an equal increase in SPL to the overall level increase, as stated previously, this frequency band tends

to be less significant to an occupant's perception of wind noise on-road as this frequency band is dominated by road noise.

Since flow speed increases over a vehicle generally show a broadband increase in aeroacoustic noise, the behaviour of the various third-octave bands is closely related to the overall SPL increase. However, changes in yaw angle will result in fluctuations more localised toward certain frequency bands and therefore deviating from this behaviour. For fluctuations in yaw angle in a leeward flow condition, the relationship is similar to that for flow speed variations. However, for fluctuations in a windward flow condition, as shown by Figure 16, a clearly identifiable deviation in the 4 kHz band is shown.

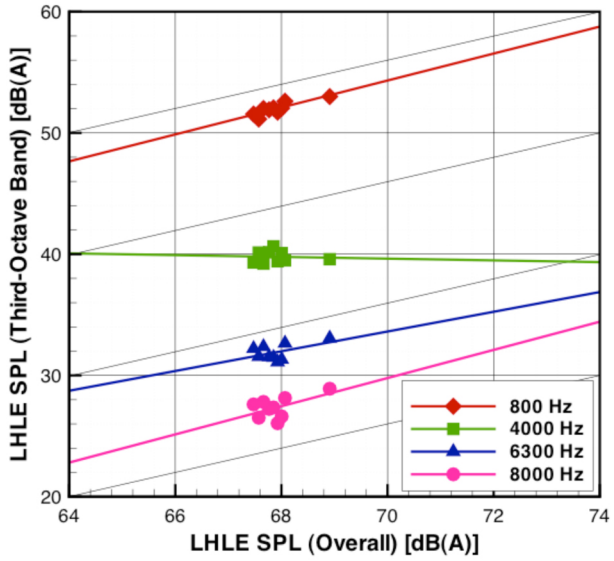

Figure 16. Comparison between third-octave and overall SPL under changes to windward yaw angle in AWT

Overall, the broadband modulation approach captures the behaviour of the third-octave frequency bands well. There is a general trend towards under-estimation of the key wind noise dominated third-octave frequency bands, and this is most likely to occur when the oncoming flow is dominated by changes in flow speed or within the leeward yaw angle range. For fluctuations in flow in the windward yaw angle range, these bands are more likely to over-predicted, particularly for the 4 kHz third-octave band.

Temporal Comparison of Measured and Predicted Cabin Noise

The results presented in this section present the results obtained using the broadband modulation approach on an example time history to compare both the quasi-steady simulated and measured signals in the time domain. The example time history was selected particularly due to the clearly identifiable change in road surface occurring after approximately eleven seconds, where the vehicle transitions between a coarser road surface to a quieter, smoother surface. This allows wind noise and road surface effects to be identified more clearly.

Figure 17, Figure 18, Figure 19, Figure 20 shows the results obtained for a number of cabin noise third-octave bands. For each graph, the on-road measured and quasi-steady wind tunnel predicted cabin noise time histories for the particular third-octave frequency band are presented and compared against the measured overall cabin noise SPL.

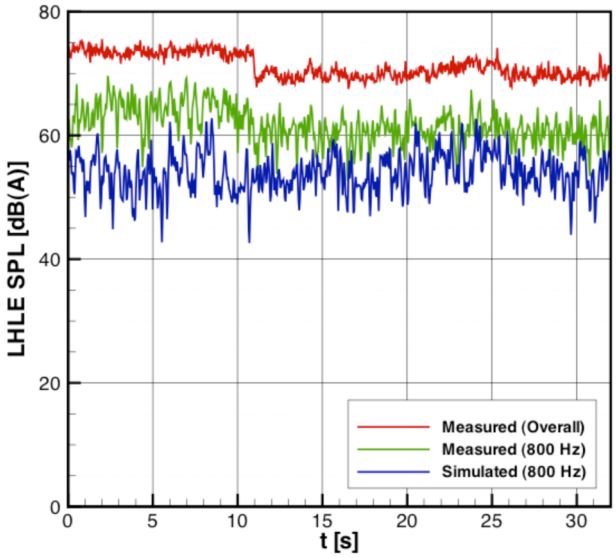

Figure 17. Temporal comparison of measured and simulated cabin noise (800 Hz)

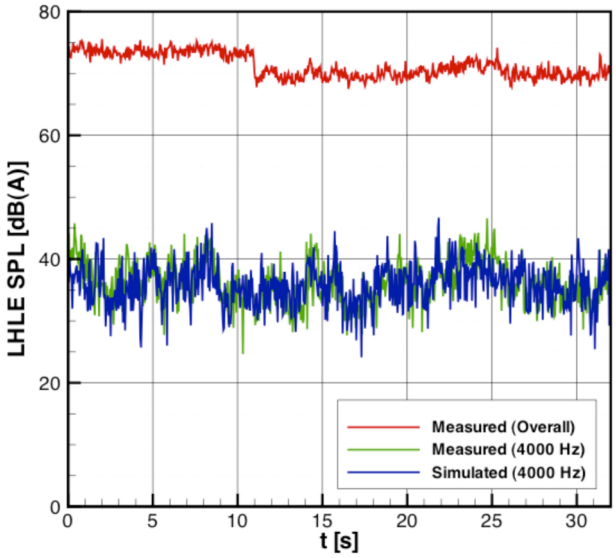

Figure 18. Temporal comparison of measured and simulated cabin noise (4000 Hz)

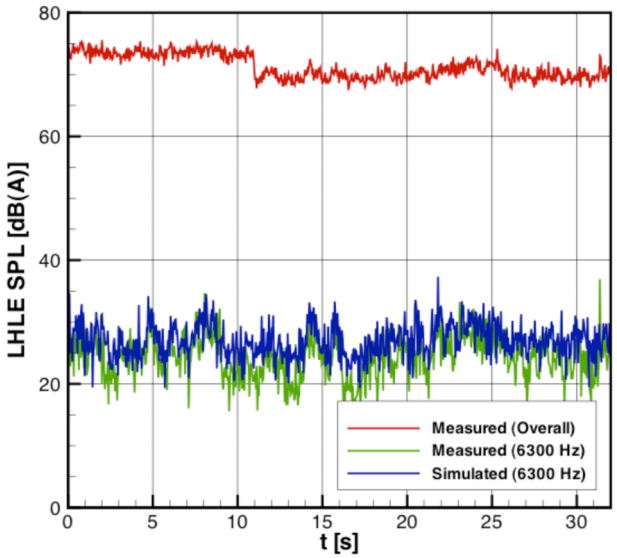

Figure 19. Temporal comparison of measured and simulated cabin noise (6300 Hz)

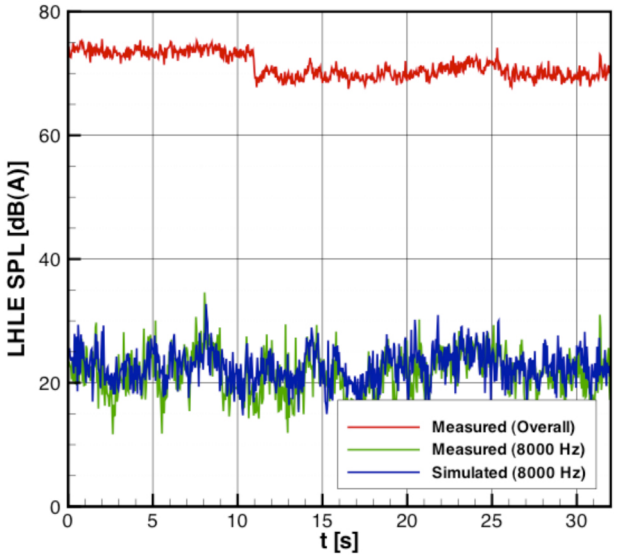

Figure 20. Temporal comparison of measured and simulated cabin noise (8000 Hz)

As previously shown, the 800 Hz third-octave band is dominated by road noise and this is shown by Figure 17. Comparing the overall SPL with the on-road measured 800 Hz band, the road surface transition is clearly identifiable. Since the road noise is independent of the oncoming flow conditions (and indeed unrelated to the wind noise contribution to the overall cabin noise), this transition is not captured by the simulated cabin noise.

Also from Figure 17, the predicted wind noise SPL is between 10-15 dB below the measured cabin noise SPL for this frequency band. Helfer and Wiedemann (2006) [20] noted that as a rule-of-thumb, AWT background noise should be around 10 dB below the wind noise levels of interest. This ensures that the tunnel background noise is insignificant compared to the measured wind noise of the vehicle. In the same vein, since the difference between the measured and predicted 800 Hz third-octave cabin noise is of the same order of magnitude owing to the road noise contribution in the measured cabin noise, it may be argued that the wind noise fluctuations in this band will be well masked and unlikely to be perceived by the occupants of the vehicle.

For the wind noise dominated frequency bands, presented by Figure 18, Figure 19, Figure 20, the correlations between the measured and predicted signals is much stronger. A visual inspection of the 30 s time traces shows good agreement but does not really make it possible to compare the two traces for timescales much less than 1 s.

Transfer Functions

To fully compare the cabin noise response of the vehicle to oncoming flow unsteadiness, the transfer function H(f) was calculated, allowing a comparison of the magnitudes of the measured and quasi-steady predicted signal to be determined at the range of fluctuation frequencies, thereby assessing the validity of the quasi-steady environment in capturing the response to oncoming flow unsteadiness. Figure 21 shows the result of this process, with each of the four third-octave frequency bands presented.

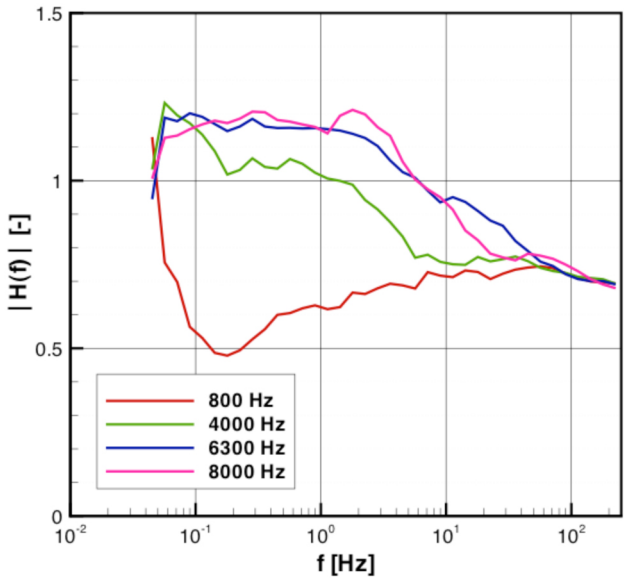

Figure 21. On-road to AWT cabin noise transfer functions

The transfer function resulting from the broadband modulation technique of Figure 21 appears to be quite different from that based on the instantaneous AWT characteristic method presented by Figure 12. To compare these transfer functions more closely, and to explain the different features, the transfer functions are divided into three key sections:

'Steady-State' Lowest Frequency Point

The first, lowest frequency points on both transfer functions relates to the time-averaged cabin noise ratio between the measured on-road data and the wind tunnel data. Since the transfer function is ratio of the on-road data divided by the wind tunnel simulated data, the 800 Hz frequency band, dominated by road noise, is significantly greater than unity. The wind noise dominated higher frequency third octave bands are much closer to unity, since the time-averaged cabin noise content in these frequency bands is similar between the two environments. Since the two simulation techniques do not generally affect the time-averaged cabin noise, this 'steady-state' point is approximately the same for both transfer functions of Figure 12 and Figure 21.

Low Frequency Content (f < 5 Hz)

As previously shown by Figure 12, the transfer function amplitude of the non-broadband modulated technique is very close to unity up to approximately 5 Hz for the wind noise dominated high frequency content. However, for the broadband modulated technique, the transfer function amplitude is up to 20% higher, indicating a greater amplitude of cabin noise fluctuations measured on-road than predicted using the broadband simulation technique.

The same transfer functions are presented in Figure 22, with a dB scale relative to the steady-state SPL as measured in the AWT. This is perhaps a more natural method of presenting ratios of SPL measured in dB. From this, it can be seen that a 20% increase in transfer function magnitude relates to an approximate increase in SPL of 5 dB.

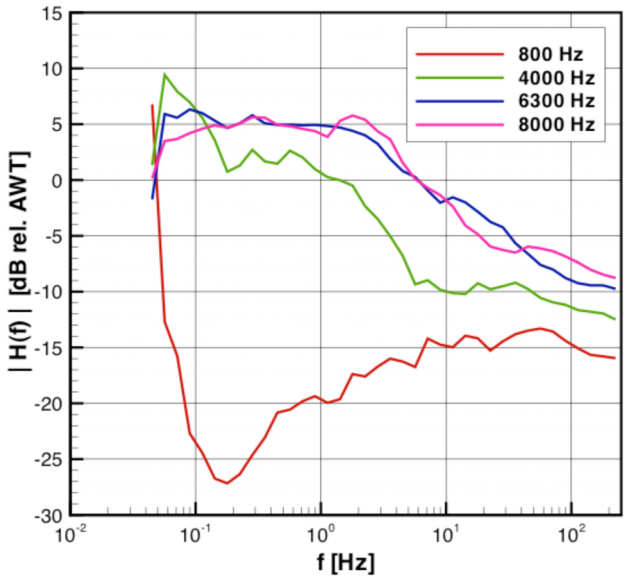

Figure 22. On-road to AWT cabin noise transfer functions (dB scale)

The greater-than-unity transfer function is expected from the broadband modulation technique itself. Figure 15 shows that the higher frequency third-octave bands show an increased sensitivity to changes in oncoming flow speed, where the vehicle responds more greatly to changes in flow speed at these higher frequencies, than the overall SPL. This results in the broadband modulation technique under-predicting the simulated cabin noise. The transfer function method used to compare both the measured and quasi-steady predicted cabin noise is the quotient of the measured over the predicted signals. Therefore, under-estimation of the predicted cabin noise will lead to an increase in the transfer function amplitude.

Since the resulting transfer function amplitude is correspondingly greater. This effect is clearer with the higher frequency 6.3 and 8 kHz bands, which in turn show greater sensitivity in Figure 15 than the 4 kHz band. This does not explain the low-frequency peak in the 4 kHz transfer function, although this is likely to be due to non-linear yaw angle effects affecting each third-octave frequency band differently when faced with a particular set of oncoming on-road flow conditions. The 800 Hz road noise band is comparatively unchanged between simulation techniques.

However, since the transfer function amplitudes are relatively constant in the low-frequency range, it is likely that this recorded deviation from quasi-steady behaviour was due to the broadband prediction technique rather than the response of the vehicle, which is likely to remain quasi-steady for the wind noise dominated cabin noise content.

High Frequency Content (f > 5 Hz)

As expected, the most significant difference in the transfer functions between the broadband modulation technique and the linearized AWT characteristic method occurs for the higher modulation frequencies (> 5 Hz). The previous self-excited effects were removed and the expected progressively decreasing transfer function amplitude is present at fluctuation frequencies greater than 2-5 Hz. As stated previously, at these higher frequencies the magnitude of the transfer functions gradually decreases as the smaller fluctuations of the oncoming flow unsteadiness have a progressively reduced impact on fluctuations in noise as heard inside the cabin.

Remarks on the Unsteady Vehicle Response

Two techniques were presented, providing information on the unsteady cabin noise response of the vehicle to oncoming flow unsteadiness. The first technique, based on purely the steady-state cabin noise response from the wind tunnel, shows a strongly quasi-steady response up to between 2-5 Hz fluctuation frequency. However, above this, the transfer function was corrupted by self-excited content.

An alternative technique was presented to remove the effects of this self-excited unsteadiness on the transfer

function; using the steady-state wind tunnel characteristic to modulate a nominal sample of cabin noise. It was found that above approximately 5 Hz, the amplitude of the transfer function decreased as the higher frequency content in the oncoming flow had a progressively reducing impact on the noise heard inside the cabin. Owing to the limitations of the broadband technique in that it does not discriminate between the various cabin noise frequency bands, the lower-frequency response did not show the clear quasi-steady behaviour of the previous technique.

However, the combination of both techniques provides useful information as to the unsteady cabin noise response of the vehicle to fluctuations in the oncoming flow. Overall, it has been shown that the cabin noise response of the vehicle to unsteadiness in the oncoming flow remains approximately quasi-steady up to between 2 and 5 Hz, after which the response decreases owing to the levels of energy in the smaller-scale oncoming fluctuations having a progressively smaller impact on noise inside the cabin. Simultaneously, the self-excited fluctuations in this higher frequency range tend to dominate, independently of transient effects in the oncoming flow conditions.

An additional benefit of the broadband modulation approach is that simulated wind noise can be generated, allowing jury testing to take place. This can be used to assess the subjective response of various vehicle characteristics, allowing the development of metrics to capture the dynamic cabin noise spectral response of vehicles to various on-road flow conditions.

A refinement to the broadband modulation technique, potentially improving the accuracy of the lower frequency response would be to modulate each third-octave band separately. This would first require a filtering technique to extract each individual band. The steady-state response of each band could then be applied to the filtered signal, ensuring that the steady-state behaviour of each band was correctly captured, potentially leading to an overall more accurate simulation. Care however must be taken in the filtering, modulation and subsequent re-mixing of each of the frequency bands such that no spectral artefacts are introduced.

CONCLUSIONS

• Conventional admittance functions relating oncoming flow yaw angle to cabin noise response are generally not suitable due to the non-linear steady state characteristics obtained in the wind tunnel. Therefore an alternative approach was used based on instantaneous conditions to determine a quasi-steady predicted cabin noise time-history. By comparing this signal with the actual transient cabin noise measured on-road, a transfer function was generated to compare the two signals and thus the applicability of a quasi-steady technique in predicting the unsteady cabin noise response.

• The cabin noise response generally remained quasi-steady for the wind noise dominated higher frequency bands up to fluctuation frequencies of between 2 and 5 Hz. At higher fluctuations frequencies, self-excited effects corrupted the transfer function and an alternative technique was developed to remove this.

• Using broadband modulation of the nominal cabin noise recorded in the wind tunnel, a technique was developed to better handle the modulation of wind noise by self-excited unsteadiness. Subsequent transfer functions showed an expected roll-off at higher frequencies, although TF amplitudes at lower frequencies were generally greater than unity as a result of the prediction technique applying the same modulation to all 3rd octave bands. An improved method is proposed to improve the measured response in the lower frequency range.

• Overall, two approaches were used to demonstrate that the cabin noise response to oncoming flow unsteadiness remained generally quasi-steady up to fluctuation frequencies of approximately 2 to 5 Hz, where above this smaller flow scales have a progressively smaller impact on cabin noise fluctuations.

Applications to Vehicle Development

From a cabin noise perspective, a quasi-steady response allows a simulation technique to be developed using steady-state cabin noise data measured in a wind tunnel and example on-road flow conditions. This makes it possible to allow different vehicles to be assessed as if they were experiencing the same windy environment. Whilst no more information is created, a better understanding of a vehicle's performance is provided including by making it possible to perform subjective tests on different vehicles subjected to identical unsteady on-road conditions. This in-turn facilitates the development of unsteady wind noise metrics to capture and compare various vehicle responses to unsteady conditions.

CONTACT INFORMATION

Nicholas Oettle
Jaguar Land Rover
noettle@jaguarlandrover.com

Dr David Sims-Williams
School of Engineering and Computer Sciences
Durham University
d.b.sims-williams@durham.ac.uk

ACKNOWLEDGMENTS

The authors are grateful to Jaguar Land Rover in supporting this work and for permission to publish, to EPSRC and SCAST for supporting the authors, to the staff at Pininfarina for supporting the wind tunnel test portion of the work and to the paper reviewers.

DEFINITIONS/ABBREVIATIONS

AWT - Aeroacoustic Wind Tunnel

C_P - Pressure Coefficient

SPL - Sound Pressure Level

REFERENCES

1. Howell, J., "An Estimation of the Unsteady Aerodynamic Loads on a Road Vehicle in Windy Conditions," SAE Technical Paper 2004-01-1310, 2004, doi:10.4271/2004-01-1310.
2. Mankowski, O. A. (2013) The Effect of Transient Airflow for Automotive Aerodynamics, PhD Thesis, Durham University.
3. Mansor, S, Passmore, M, "Estimation of bluff body transient aerodynamics using an oscillating rig" Journal of Wind Engineering and Industrial Aerodynamics 96:1218-1231, 2008.
4. Mayer, J., Schrefl, M., and Demuth, R., "On Various Aspects of the Unsteady Aerodynamic Effects on Cars Under Crosswind Conditions," SAE Technical Paper 2007-01-1548, 2007, doi:10.4271/2007-01-1548.
5. Ryan, A. and Dominy, R., "The Aerodynamic Forces Induced on a Passenger Vehicle in Response to a Transient Cross-Wind Gust at a Relative Incidence of 30°," SAE Technical Paper 980392, 1998, doi: 10.4271/980392.
6. Wordley, S. J., On-road turbulence. PhD thesis, Monash University, 2009.
7. Sims-Williams, D., "Cross Winds and Transients: Reality, Simulation and Effects," *SAE Int. J. Passeng. Cars - Mech. Syst.* 4(1):172-183, 2011, doi:10.4271/2011-01-0172.
8. Lindener, N., Miehling, H., Cogotti, A., Cogotti, F. et al., "Aeroacoustic Measurements in Turbulent Flow on the Road and in the Wind Tunnel," SAE Technical Paper 2007-01-1551, 2007, doi:10.4271/2007-01-1551.
9. Peric, C., Watkins, S., Lindqvist, E., and Saunders, J., "Effects of On-Road Turbulence on Automotive Wind Noise: Comparing Wind-Tunnel and On-Road Tests," SAE Technical Paper 970406, 1997, doi: 10.4271/970406.
10. Oettle, N., Mankowski, O., Sims-Williams, D., Dominy, R. et al., "Assessment of a Vehicle's Transient Aerodynamic Response," SAE Technical Paper 2012-01-0449, 2012, doi:10.4271/2012-01-0449.
11. Oettle, N., Sims-Williams, D., Dominy, R., Darlington, C. et al., "The Effects of Unsteady On-Road Flow Conditions on Cabin Noise: Spectral and Geometric Dependence," *SAE Int. J. Passeng. Cars - Mech. Syst.* 4(1):120-130, 2011, doi:10.4271/2011-01-0159.
12. Oettle, N., Sims-Williams, D., Dominy, R., Darlington, C. et al., "The Effects of Unsteady On-Road Flow Conditions on Cabin Noise," SAE Technical Paper 2010-01-0289, 2010, doi:10.4271/2010-01-0289.
13. Oettle, N.R. The Effects of Unsteady On-Road Flow Conditions on Cabin Noise, PhD Thesis, Durham University, 2013.
14. Lawson, A., Dominy, R., Sims-Williams, D., and Mears, P., "A Comparison Between On-Road and Wind Tunnel Surface Pressure Measurements on a Mid-Sized Hatchback," SAE Technical Paper 2007-01-0898, 2007, doi:10.4271/2007-01-0898.
15. Irwin, H, Cooper, K, Girard, R, Correction of Distortion Effects Caused by Tubing Systems in Measurements of Fluctuating Pressures, Journal of Industrial Aerodynamics, 1979. 5(1-2), p. 93-107
16. Sims-Williams, D. and Dominy, R., "Experimental Investigation into Unsteadiness and Instability in Passenger Car Aerodynamics," SAE Technical Paper 980391, 1998, doi: 10.4271/980391.
17. Bendat, J. S. and Piersol, A. G. (1993). Engineering applications of correlation and spectral analysis. John Wiley & Sons inc., New York, second edition.
18. Schröck, D., Widdecke, N., and Wiedemann, J. Aerodynamic response of a vehicle to turbulent wind. In 7th FKFS conference "progress in vehicle aerodynamics and thermal management", Stuttgart, 2009.
19. George, A., "Automobile Aerodynamic Noise," SAE Technical Paper 900315, 1990, doi: 10.4271/900315.
20. Helfer, M. and Wiedemann, J. Design of wind tunnels for aeroacoustics. In Lecture series: experimental aeroacoustics. Von Karman Institute, Rhode-Genèse, Belgium, 2006